Fourier Transform Infrared and Quasi-Elastic Neutron Scattering Investigations on the Binding States and the Dynamics of Benzene Molecules in the Pores of MCM-41 Molecular Sieves

A. Sahasrabudhe,[†] S. Mitra,[‡] A. K. Tripathi,[†] R. Mukhopadhyay,[‡] and N. M. Gupta*[,†]

Applied Chemistry Division and Solid State Physics Division, Bhabha Atomic Research Centre, Mumbai 400 085, India

Received: July 1, 2002; In Final Form: August 12, 2002

The in-plane C−H/C−C, out-of-plane C−H, and the fundamental ν_{19} C−C stretch vibrations of benzene molecules were monitored by FTIR spectroscopy, for adsorption in MCM-41 at room temperature and at different loadings. The results were compared with the corresponding data on ZSM-5 zeolites. The frequency and the relative intensity of IR bands point to the development of a compressed state of benzene in the pores of MCM-41, the density of which depended upon loading and lay in general between that of bulk liquid and a solidlike phase formed in the pores of ZSM-5 zeolite on benzene adsorption. Quasi-elastic neutron scattering results reveal that the pore characteristics play a crucial role in deciding the dynamics of benzene molecules in a confined medium. Thus, in contrast to the molecular motions of benzene in ZSM-5 zeolite where only rotational motion was observed in the instrumental time window of 10^{-10}−10^{-12} s, the benzene molecules adsorbed in MCM-41 exhibit only translational motion. Further, the value observed for the translational diffusion constant ($D = 2.18 \times 10^{-5}$ cm^2/s) of benzene occluded at saturation in MCM-41 confirmed the existence of its condensed state. Because of the unhindered mobility in mesopores, a smaller fraction of benzene gets occluded in MCM-41 compared to ZSM-5 zeolite, under the identical conditions of loading. Also, the parallel studies using MCM-41 with different Si/Al ratios and with different charge balancing cations rule out the possibility of any specific coordination of the occluded benzene with the framework sites of molecular sieves. The results are explained in terms of the current theories of capillary condensation of fluids on confinement in narrow pores.

Introduction

The pore characteristics are known to play a key role in controlling the molecular sieving properties and the adsorption behavior of zeolitic materials. The studies on occlusion of guest molecules in porous materials are important not only because of these practical applications but also because they help in fundamental understanding of the binding states of adsorbates at a molecular level inside the confining geometries. Yet, the research activities in this area have so far concentrated either on exploring the electronic interaction of adsorbates with the framework or extraframework sites under low-temperature low-pressure conditions[1−3] or on the bulk sorption behavior of various adsorbents.[4−6] There is, at the same time, a lack of information on the nature of adsorbate−adsorbate interaction under the conditions of encapsulation in zeolite pores. It is widely reported that the thermodynamic and transport properties of fluids are considerably altered on their physical confinement in a well-defined channel and cavity system of porous materials. Thus, the capillary condensation of gases to a liquid form and a change in the temperature of phase transformation in the case of liquids adsorbed in ultrasmall pores are some of the well-reported phenomena.[5−7] In addition to the physicochemical characteristics of confining medium, the critical size and the configuration of sorbate molecules are also known to influence these processes considerably.[8,9] At the same time, the interaction of small adsorbate molecules with the framework sites, hydroxy groups, charge balancing cations, and the extraframework aluminum sites, etc., has been demonstrated in a number of publications.[10−12] In the previous studies reported from this laboratory,[13−19] we employed FTIR spectroscopy and quasi-elastic neutron scattering (QENS) methods with the objective of monitoring the state of guest molecules occluded in zeolitic cavities at temperatures of ambient and above, and also under the varying conditions of pressure. In these studies we demonstrated that small molecules such as CO, CO_2, benzene, and cyclohexane existed in a clustered state when occluded at room temperature in microporous zeolites of X-, Y- and ZSM-5 type. Small changes in the pore size of these materials on cation exchange resulted in significant modification in the vibrational modes of these molecular clusters.[16,17] To further explore the influence of pore size on the adsorption process, we have now employed FTIR and QENS techniques so as to monitor the molecular motions and the binding states of benzene molecules on entrapment in the pores of MCM-41 molecular sieves at room temperature. The effect of various parameters, such as the Si/Al ratio, loading of adsorbate, and nature of charge balancing cation, has been monitored. Some comparative data on NaZSM-5 have been included to discriminate between the roles of a hexagonal array of uniform mesopores in MCM-41 versus the intersecting microporous three-dimensional channel system of ZSM-5 zeolite.[19]

Experimental Section

The MCM-41 sample (Si/Al ratio ∼30) used in this study was synthesized by a conventional hydrothermal route, fumed

* Corresponding author E-mail: nmgupta@magnum.barc.ernet.in. Fax: 091-22-5505151.

[†] Applied Chemistry Division.

[‡] Solid State Physics Division.

10.1021/jp021545d CCC: $22.00
Published on Web 09/28/2002

silica and Al-isopropoxide being the sources of Si and Al, respectively. Cetyltrimethylammonium bromide (CTAB) was employed as a structure-directing agent, and NaOH was used for precipitation. XRD, IR, and TG methods confirmed the identity of MCM-41. The N_2 adsorption surface area, pore size, and pore volume of a calcined sample were evaluated to be around 1000 $m^2\ g^{-1}$, 34 Å, and 0.68 $cm^3\ g^{-1}$, respectively. A template free NaZSM-5 zeolite ($SiO_2/Al_2O_3 = 40$, surface area 454 $m^2\ g^{-1}$, and pore volume 0.26 $cm^3\ g^{-1}$) was obtained from the Research and Consultancy Directorate of the ACC Ltd., Thane, India.

A stainless steel IR cell used in this study has the facility for evacuation, pretreatment of a sample at variable conditions of temperature and pressure, and introduction of a desired amount of an adsorbate.[13,14] A Mattson model Cygnus-100 FTIR spectrophotometer equipped with a DTGS detector was used in transmission mode, and 300 scans were co-added at a resolution of 4 cm^{-1} for plotting of each spectrum. The sample wafer (2.5 cm diameter, ~70 mg) was subjected to a pretreatment at 350 °C (24 h, 1.3×10^{-3} mbar), cooled to ambient temperature, and then exposed to a desired amount of benzene (1−11 mmol g^{-1}). For these doses, when introduced into the evacuated IR cell without a sample, benzene was in a vapor form and the pressure in the cell varied in the range 6−60 mbar. Unless mentioned otherwise, IR spectra were plotted with the spectrum of an unexposed sample wafer as reference so as to compensate for the framework vibrations. The IR bands due to residual vapor in the cell were finally subtracted from the IR spectrum of a sample wafer exposed to benzene, and the data in general represent such subtracted spectra, unless mentioned otherwise. Spectra were also plotted independently after introducing gaseous and liquid (placed between two CsI windows) forms of benzene in the IR cell, sans a sample wafer, and these data are included for a ready reference. The values given in parentheses in some of the figures indicate the value of absorbance, taken as a measure of relative intensity. Frequency reproducibility of individual IR bands was of the order of 1−2 wavenumbers during repeated experiments. High-purity grade benzene was double distilled over sodium benzophenone before use.

Quasi-elastic neutron scattering (QENS) data were collected prior to and after room-temperature adsorption of benzene in MCM-41 molecular sieves, after a pretreatment (625 K, 48 h) under vacuum (1.3×10^{-6} mbar). The amount of benzene adsorbed was around 10 mmol g^{-1}. The experiments were performed using an incident neutron beam of 4 Å wavelength, and the energy resolution of the neutron spectrometer was 200 μeV. The neutron scattering data on benzene were recorded in a Q-range of 0.8−1.8 $Å^{-1}$. The spectrometer is used in multiangle reflecting crystal (MARX) mode where one essentially uses a combination of a large analyzer crystal and a linear position sensitive detector, providing larger throughput. PG crystals are used for both the double monochromator and analyzer. Further experimental details may be found elsewhere.[19,20]

Results

In-Plane C−H/C−C Stretching Vibrations. Spectrum a in Figure 1 shows the IR bands due to fundamental C−H stretching (ν_{20}) and combination C−C stretching vibrations of benzene when adsorbed (4.47 mmol g^{-1}) in an MCM-41 sample at room temperature. The corresponding amount of benzene in the IR cell in the absence of a sample gave a typical spectrum of gas phase benzene, as shown in Figure 1b. Appropriate subtraction

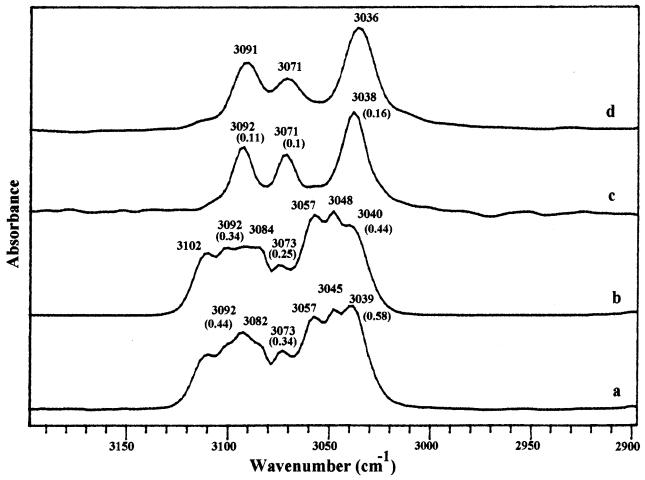

Figure 1. (a) C−H stretching (ν_{20}) and combination C−C stretching vibrations of benzene when dosed (4.47 mmol g^{-1}) over the MCM-41 wafer. (b) IR spectrum in this region when the same amount of benzene was introduced in the cell without a sample. (c) Subtraction spectrum (b) − (a). Spectrum (d) shows typical IR bands of liquid benzene in this region.

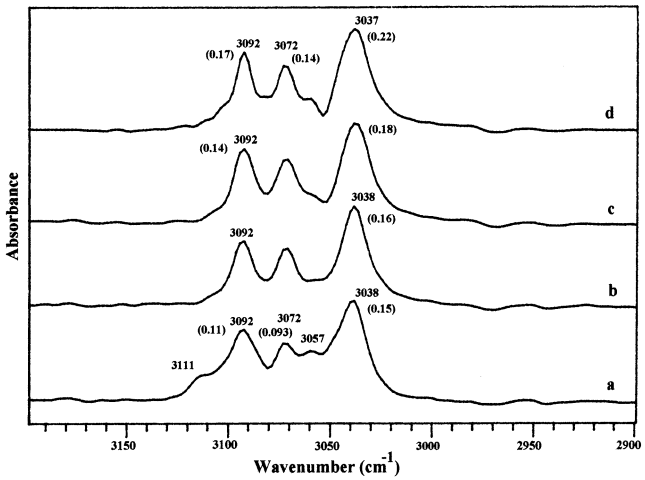

Figure 2. Subtracted spectra as in Figure 1, showing the effect of loading on C−H stretching and combination C−C stretching vibrations of benzene adsorbed in MCM-41: (a) 2.23, (b) 4.47, (c) 8.95, and (d) 11.0 mmol g^{-1}.

of IR bands of Figure 1b from that in Figure 1a gave the vibrational bands due to adsorbed species, and a typical subtraction spectrum is given in Figure 1c. A comparison shows the complete absence of PQR branches in Figure 1c that are characteristic of vapor phase benzene (cf. Figure 1b), and the spectrum of occluded benzene matches largely with that of its liquid phase. A typical spectrum of liquid benzene in this region is shown in Figure 1d, for comparison.

When monitored as a function of time, the intensity of IR bands in Figure 1c reached saturation within the few minutes of introduction of benzene. The intensity of the individual bands, however, increased progressively with increasing benzene dose, as shown in Figure 2. As indicated by the absorbance values given in this figure, the dose dependent variation was almost uniform for all the individual vibrational bands; the increase in the intensity being around 27 and 50% for the increase in benzene loading from 2.23 to 8.95 and 11 mmol/g, respectively (Figure 2c,d). The presence of weak bands, at 3111 and 3057 cm^{-1}, in Figure 2a and a comparison with Figures 1b and 1d suggest that the benzene in this case existed in a phase that matched neither the liquid or the vapor forms. For still lower

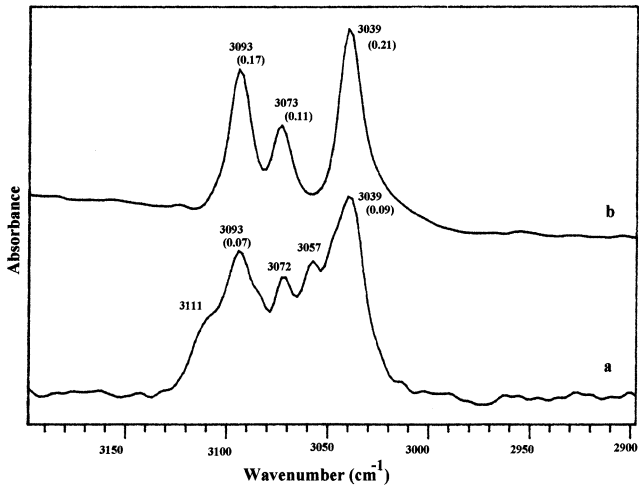

Figure 3. Comparative subtraction IR spectra in ν(C−H) and ν(C−C) regions for exposure of 0.98 mmol of benzene per gram of (a) MCM-41 and (b) NaZSM-5 samples.

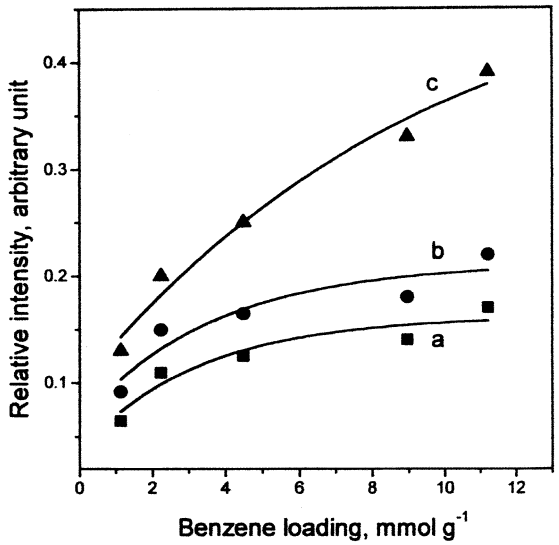

Figure 4. Growth behavior of (a) 3092, (b) 3038, and (c) 1479 cm^{-1} vibrational bands as a function of benzene loading.

loadings, the amount of benzene sorbed was relatively small and the above-mentioned IR bands at 3111 and 3057 cm^{-1} were more intense. Spectrum a in Figure 3 presents the IR spectrum of MCM-41 exposed to 0.98 mmol/g of benzene at room temperature. Corresponding spectrum for adsorption of benzene in NaZSM-5 is given in Figure 3b. It is noticed that the absorbance of different IR bands is greater by a factor of at least 2 in case of adsorption of benzene in NaZSM-5 (Figure 3b), as compared to that in MCM sample (Figure 3a). Also, the nature of the IR spectrum of benzene is different in two cases, suggesting that it existed in different states when adsorbed in ZSM and MCM samples under identical conditions.

The growth of some prominent bands as a function of benzene loading in MCM-41 is plotted in curves a and b of Figure 4. These data indicate that the process of pore filling may occur in two stages, initially fast and then at a slow rate.

Fundamental ν_{19} C−C Stretching Vibration. As in the case of combination IR bands shown in Figure 2, the intensity of the fundamental C−C stretching band at 1479 cm^{-1} increased progressively with loading, as shown in Figure 5A. Again, the intensity of this band was smaller for adsorption in MCM-41 compared to NaZSM-5 under identical loading conditions. The comparative ν_{19} C−C stretching vibrational band of benzene

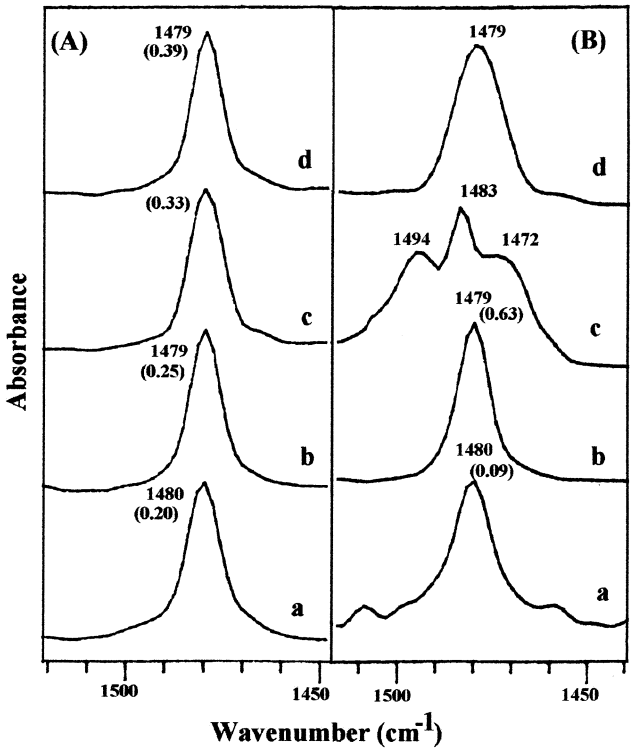

Figure 5. (A) Fundamental C−C stretching (ν_{19}) vibration of benzene, dosed in different amounts over the MCM-41 molecular sieve: (a) 2.23, (b) 4.47, (c) 8.95, and (d) 11.19 mmol g^{-1}. (B) Comparative study of the in-plane ν_{19} vibrational band for exposure of 0.98 mmol g^{-1} benzene over (a) MCM-41 and (b) NaZSM-5 samples Spectra c and d show comparative vibrational bands of gaseous and liquid benzene, respectively.

for adsorption (0.98 mmol g^{-1}) in NaZSM-5 and NaMCM-41 are plotted in Figure 5B. As seen from the value of absorbance, the amount of benzene occluded in MCM-41 is smaller by a factor of around 7 compared to the amount adsorbed in ZSM-5 under identical conditions. It is also of interest to notice that even for small amounts of benzene occluded in MCM, we see no PQR separation in the ν_{19} vibrational band (spectrum a, Figure 5B). For comparison, IR bands in this region for vapor and liquid phases of benzene are included in Figure 5B (curves c and d). This indicates that even when adsorbed in a small amount, benzene inside the pores of MCM existed in a phase different from that of benzene vapor. The growth behavior of the 1479 cm^{-1} band was similar to that of in-plane vibrational bands mentioned above, and the typical data are plotted in curve c of Figure 4.

Out-of-Plane C−H Vibration. A considerable difference was noticed in the IR spectra in this region for adsorption of benzene in MCM-41 and NaZSM-5 samples. Plots showing this comparison for a benzene dose of 2.2 mmol g^{-1} in each case are given in spectra a and b of Figure 6. Curves c and d of this figure show the IR spectra of vapor and liquid phases of benzene, respectively, recorded without a sample wafer in the IR cell. It is of interest to notice the presence of multiple overlapping bands in the case of the benzene adsorbed in NaZSM-5 zeolite (spectrum b). Thus, instead of 1960 cm^{-1} bands in Figure 6d, we observe a set of four vibrations, i.e., 2006, 1979, 1969, and 1956 cm^{-1}, and similarly four vibrations at 1873, 1850, 1836, and 1812 cm^{-1} are observed in lieu of the 1815 cm^{-1} band of liquid benzene (Figure 6b). On the other hand, IR bands at 1969 and 1823 cm^{-1}, in addition to weak shoulder bands at ∼1950 and 1801 cm^{-1}, were observed for the benzene adsorbed in MCM-41 (Figure 6a). Again, very weak

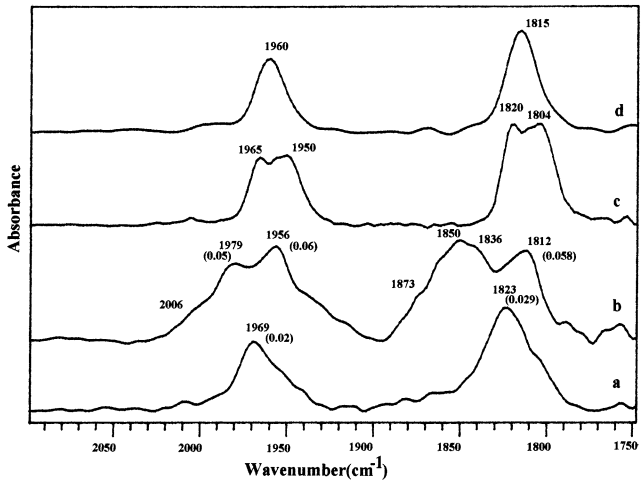

Figure 6. C−H out of plane vibrational bands when 2.23 mmol of benzene was dosed per gram of (a) MCM-41 and (b) NaZSM-5. Spectra c and d show the vibrational bands in this region for vapor and liquid forms of benzene, respectively.

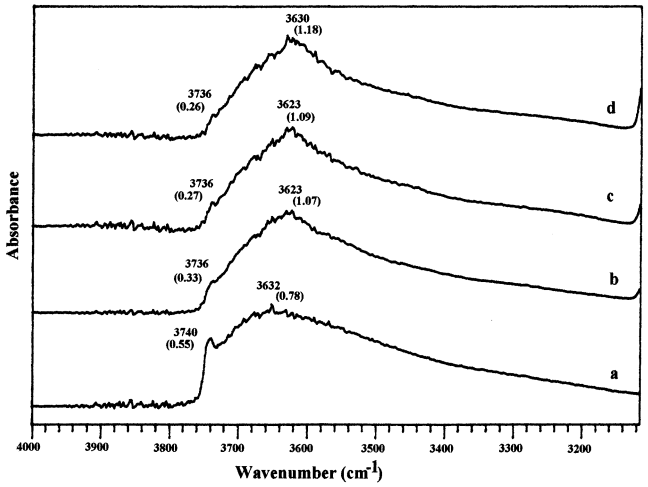

Figure 7. ν(OH) vibrational bands of MCM-41 (plotted with air as reference), prior to (spectrum a) and after exposure to different amounts of benzene at room temperature: (b) 2.2, (c) 8.9, and 11.2 mmol g^{-1}.

vibrational bands were observed in this region, for smaller loadings of benzene in MCM-41, indicating the occlusion of a negligibly small amount of benzene. On the contrary, a spectrum similar to that in Figure 6b was observed for a loading of as low as 0.1 mmol g^{-1} in the case of experiments on ZSM-5 zeolites. Also, similar to the behavior of previously mentioned IR bands, a progressive increase was observed in the intensity of different out-of-plane vibrational bands in Figure 6a, the overall spectral features remaining basically the same.

O−H Region Bands. Figure 7a presents a typical IR spectrum of MCM-41, after outgassing at 625 K (24 h) and cooling to ambient temperature. This spectrum, recorded with air as reference, is similar to that reported in the literature[21] and exhibits a prominent band at 3740 cm^{-1} due to isolated silanol groups, in addition to an unresolved broad absorbance band peaking at around 3632 cm^{-1}. Spectra b−d in this figure represent the IR data for exposure of a sample wafer to different amounts of benzene in the range of 2−11 mmol g^{-1}. As seen clearly, the main effect of benzene loading is a progressive decrease in intensity of the 3740 cm^{-1} band whereas its frequency increased by ca. 4 cm^{-1}. At the same time a new broad band appears at ∼3623 cm^{-1}, the other spectral features remaining the same. It is important to notice that no bands are observed in the lower ν(OH) region (i.e., 3500−3000 cm^{-1}), in contrast to a widely reported observation in the case of loading of hydrocarbons in microporous zeolites, such as HZSM5.[19,22]

Effects of Postexposure Evacuation, Si/Al Ratio, and Cation Exchange in Molecular Sieves. The vibrational bands mentioned above were removed almost completely when an MCM sample exposed to benzene, irrespective of its loading, was outgassed for a few minutes. On the other hand, the binding of benzene in ZSM-5 channels was very strong and only a small fraction was removed even after 1 h of evacuation.[18,19]

Also, the vibrational bands similar to those described above were observed when an all-silica MCM-41 sample was employed for benzene adsorption. The only difference was that the intensity of the IR bands was marginally greater, and that was related to a larger pore volume of the material. Similarly, no significant change was observed in the frequency and the nature of the vibrational bands of benzene when MCM-41 exchanged with a group IIA cation was used as the host material. The marginal difference was seen only in the values of absorbance and the amount of occluded benzene.

Quasi-Elastic Neutron Scattering. In a neutron scattering experiment the scattered intensity is analyzed as a function of both energy and momentum transfer $Q = (4\pi \sin \theta/\lambda)$, where 2θ is the scattering angle. The quantity measured is the double differential scattering cross section ($d^2\sigma/\partial E \partial\Omega$), which represents the probability that a neutron is scattered with energy change dE into the solid angle $d\Omega$.[23]

$$\frac{d^2\sigma}{\partial\omega\partial\Omega} \propto \frac{\mathbf{k}}{\mathbf{k}_0}[\sigma_{coh}S_{coh}(\mathbf{Q},\omega) + \sigma_{inc}S_{inc}(\mathbf{Q},\omega)] \qquad (1)$$

$S(\mathbf{Q},\omega)$ is known as the scattering law and the subscripts "coh" and "inc" denote the coherent and incoherent components. $\mathbf{k}$ and $\mathbf{k}_0$ are the final and initial wave vectors. $\mathbf{Q} = \mathbf{k} - \mathbf{k}_0$ is the wave vector transfer and $\hbar\omega = E - E_0$ is the energy transfer. Incoherent scattering involves the same nucleus at two successive times, so there are no interference effects between the amplitudes scattered by different nuclei, whereas in coherent scattering, the total intensity observed results from the sum of the different intensities scattered from the individual nuclei. In hydrogenous systems, such as benzene, total scattering is dominated by the incoherent scattering of protons as σ_{coh}(any element) $\ll \sigma_{inc}$(proton). So in case of hydrogenous systems,

$$\frac{d^2\sigma}{\partial\omega\partial\Omega} \propto \frac{\mathbf{k}}{\mathbf{k}_0}[\sigma_{inc}S_{inc}(\mathbf{Q},\omega)] \qquad (2)$$

In general, the incoherent scattering law can be written as[24]

$$S_{inc}(\mathbf{Q},\omega) \propto A(\mathbf{Q})\,\delta(\omega) + [1 - A(\mathbf{Q})]\,L(\Gamma,\omega) \qquad (3)$$

where the first term is the elastic part and the second term is the quasi-elastic part. $L(\Gamma,\omega)$ is a Lorentzian and Γ is the half-width at half-maximum (HWHM) of the Lorentzian function inversely related to the time constant of the motion. It is convenient to analyze the data in terms of the elastic incoherent structure factor (EISF), which provides the information about the geometry of the molecular motions. If $I_{el}(\mathbf{Q})$ and $I_{qe}(\mathbf{Q})$ are the elastic and quasi-elastic intensities respectively, the EISF is defined as[23]

$$\text{EISF} = \frac{I_{el}(\mathbf{Q})}{I_{el}(\mathbf{Q}) + I_{qe}(\mathbf{Q})} \qquad (4)$$

Therefore, $A(\mathbf{Q})$ in eq 3 is nothing but the EISF.

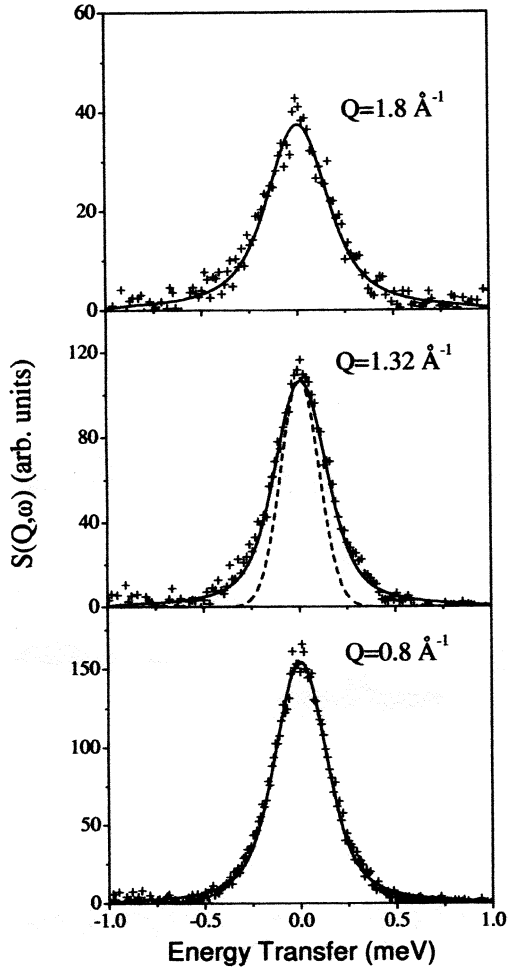

Figure 8. QENS data at some typical Q values for adsorption of benzene in MCM-41, fitted with a Lorentzian. The solid and dotted lines represent the fit and the resolution function, respectively.

The QENS spectra from the dehydrated MCM-41 did not show any further broadening over the resolution function of the instrument. However, significant broadening was observed from the sample loaded with benzene and this may therefore be attributed exclusively to the molecular motions of benzene. To explore the contribution of occluded benzene, the QENS spectrum of bare molecular sieves was subtracted from the spectrum of the loaded sample. The data thus obtained were analyzed following an unbiased procedure, where no specific model was assumed. Elastic and quasi-elastic components in the total spectra at all **Q** values were estimated. The model scattering law given in eq 3 was convoluted with the instrumental resolution and the parameters (A(**Q**) and Γ) were determined by least-squares fit to the data. The elastic and quasi-elastic parts were separated from the total spectra. The data in Figure 8 show that the elastic component (A(**Q**)) is almost zero for all the **Q** values, suggesting that the observed dynamics does not involve any elastic part and one Lorentzian function explains the data quite well. This indicates that the observed QE broadening corresponds only to the translational motion of benzene molecules. The rotation of the benzene molecules could be either very fast or very slow to be observed in the time domain of the present measurements. The HWHM values of the Lorentzian function as obtained from the fit are given in Figure 9. To arrive at an understanding of the dynamics of benzene molecules in the pores of MCM-41, we now compare these data with some plausible models. When a molecule, such as benzene, performs translational motion in a confined space,

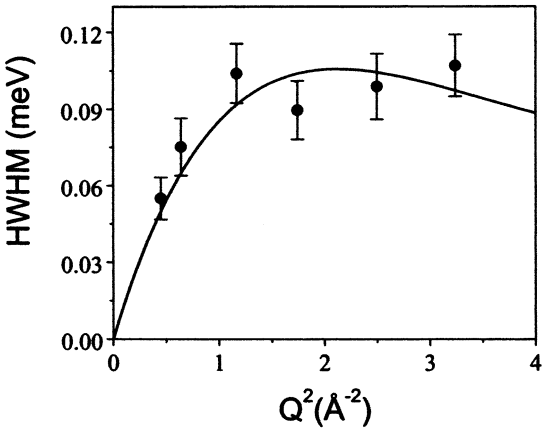

Figure 9. Variation of HWHM with Q^2. The solid line represents a fit with the Chudley−Elliott model.

different models can be envisaged to describe its motion. The most simple motion that can be thought of is the Brownian motion, where it is assumed that the particles move under the influence of the forces arising from the collisions between them. The particles move in a straight line between two collisions. After a collision the particle goes to another random direction, independent of the previous one. In this case, incoherent scattering law can be calculated by solving Fick's law[23] and written as

$$S_{\mathrm{inc}}(\mathbf{Q},\omega) = \frac{1}{\pi}\frac{D\mathbf{Q}^2}{\omega^2 + (D\mathbf{Q}^2)^2} \tag{5}$$

The scattering law exhibits a Lorentzian shape whose HWHM increases with the momentum transfer according to a $D\mathbf{Q}^2$ law and provides a direct method of determining the diffusion constant.

In the case of Brownian motion, the jump length l of the diffusion particle is assumed to be small compared to the distance $|\mathbf{r}|$ of this particle from the origin. In other words, diffusion is assumed to occur via infinitely small, elementary jumps. This assumption is satisfied if we are concerned only at small **Q** values where the exact mechanisms of diffusion are not revealed and Fick's law is satisfied. At large momentum transfer, the continuous diffusion model is no longer true and we need to describe the diffusion process in more detail. One such model was formulated by Chudley and Elliott.[25] This model assumes that for a time interval τ, an atom remains on a given site, vibrating about a center of equilibrium, building up a thermal cloud. After this time, the atom moves rapidly to another site, in a negligible jump time. The jump length l is assumed to be the same for all such jumps under consideration. This model is also called a fixed jump model. The powder-averaged scattering law in this case can be written as

$$S_{\mathrm{inc}}(\mathbf{Q},\omega) = \frac{1}{\pi}\frac{\Gamma(\mathbf{Q})}{\omega^2 + (\Gamma(\mathbf{Q}))^2} \tag{6}$$

where

$$\Gamma(\mathbf{Q}) = \frac{1}{\tau}\left[1 - \frac{\sin \mathbf{Q}l}{\mathbf{Q}l}\right] \tag{7}$$

One can also find out the diffusion constant, D, from Einstein's relation

$$D = \frac{l^2}{6\tau} \tag{8}$$

In Figure 9 are shown the fit of the HWHM values of the Lorentzians as per the Chudley−Elliott model. As seen in Figure 9 the experimental values fit quite well with this model. The values of residence time (τ), jump length ($\langle l \rangle$) and the diffusion constant (D) obtained from the fitting in Figure 9 are found to be 7.53 ± 0.60 ps, 3.14 ± 0.32 Å, and (2.18 ± 0.61) × 10^{-5} cm^2/s, respectively. On comparing this D value with the value reported for the diffusion constant of liquid benzene at 298 K ($D = (2.21 \pm 0.21) \times 10^{-5}$ cm^2/s),[26,27] we may conclude that the translational diffusion constant of benzene in MCM-41 is of the same order as that of bulk liquid benzene. The small changes in the density of this condensed phase of benzene as a result of encapsulation in MCM-41 are, however, not amenable to detection by the QENS technique.

Discussion

In a detailed discussion on this subject, and on the basis of the multiple out-of-plane C−H bending vibrations (Figure 6b) and the relative intensity of different out-of-plane and in-plane C−C/C−H stretching vibrational bands of benzene, we have demonstrated earlier that benzene molecules existed in a highly compressed (clustered) state when adsorbed in the micropores of the HZSM-5 zeolite.[18,19] Also, because no frequency shift or band splitting is found to occur in the in-plane fundamental C−H stretching (ν_{20}) and combination C−C vibrations of the occluded benzene molecules in the 3200−3000 cm^{-1} region and also in the fundamental ν_{19} C−C stretching vibration (1480 cm^{-1}), it has been deduced that the benzene molecules in the clustered state are packed with their plane parallel to the zeolitic walls and interact with each other through π-electron clouds.[18] Furthermore, the quasi-elastic neutron scattering results revealed in this previous study that the occluded molecules undergo a 6-fold rotation and no electronic bonding may occur between the benzene and the framework sites of zeolite.[19] The results of the present study on MCM reveal that the binding state of occluded benzene is influenced considerably by the shape/size of zeolitic pores. Following are the salient features:

1. A comparison of spectra in Figures 2a−d and 3a on one hand and Figure 1b,d on the other clearly reveals that the benzene occluded in the pores of MCM-41 undergoes a progressive transformation to a denser phase with the increase in benzene loading. The relative intensity of individual bands in Figure 3a indicate that for a low loading (∼0.98 mmol g^{-1}), benzene existed in neither the liquid or vapor phase, thus suggesting the formation of an intermediate state.

2. The condensation of benzene in the pores is further confirmed by the complete absence of PQR branches in the ν_{19} vibrational band of occluded benzene (Figure 5). The absence of these vibrations even in case of low loadings (Figure 5B, spectrum a) may be taken as evidence that the overlapping vibrational bands in Figures 2 and 3a may not arise simply due to a mixture of vapor and liquid forms of benzene.

3. The out-of-plane C−H vibrational bands in Figure 6 again present a similar picture. It is seen that the frequency and the relative intensity of the vibrational bands in Figure 6a match with neither the vapor nor the liquid phases (Figures 6c,d) indicating the development of an intermediate state.

4. This contention finds support from the widths at half-maximum (fwhm) of different vibrational bands. Thus, considering for instance the in-plane C−H/C−C stretching vibrational band, compared to a fwhm value of ∼32 cm^{-1} for benzene vapor (Figure 1b) and a corresponding value of ∼18.75 cm^{-1} for liquid benzene (Figure 1d), the value in the case of benzene adsorbed in MCM-41 is found to be ∼15 cm^{-1}. Similar observation could be made in the case of all other vibrational bands of benzene monitored in the present study. It is thus evident that the confinement in the pores of MCM-41 leads to considerable decrease in the degree of randomization of benzene molecules, giving rise to a state in which the adsorbate−adsorbate interaction is stronger than that in case of bulk liquid. Further, the width of this band is found to be ∼12.7 cm^{-1} in the case of NaZSM-5, which is in conformity with the reported behavior of benzene molecules in the pores of ZSM-5 zeolites.[18, 19]

TABLE 1: Ratio of In-Plane C−C Stretch Vibrational Band (ν_{19}) at 1479 cm^{-1} and In-Plane C−H Stretching (ν_{20}) and Combination C−C Stretching Vibrational Bands of Benzene (3093, 3039 cm^{-1}) for Adsorption at Two Typical Loadings in MCM-41 and HZSM-5[a]

	I_{1479}/I_{3093}			I_{1479}/I_{3039}		
		0.98 mmol g^{-1}	2.24 mmol g^{-1}		0.98 mmol g^{-1}	2.24 mmol g^{-1}
MCM-41		1.35	1.81		0.97	1.32
NaZSM-5		3.47	2.89		2.95	2.25
benzene vapor	0.24			0.19		
benzene liquid	1.25			0.83		

[a] The comparative values for the liquid and the gaseous phases of benzene are also included.

5. As discussed in our earlier publications, the increase in intensity ratio of the fundamental vibration (ν_{19}) at 1479 cm^{-1} and the other in-plane vibrations at 3092, 3071, and 3039 cm^{-1} is a feature associated with the transformation of benzene to a more condensed state. The typical values of frequency ratio (1479/3093 and 1479/3039) given in Table 1 clearly reveal that the benzene adsorbed in MCM-41 existed in a phase that is more dense than the bulk liquid but less than a highly compressed (solidlike) phase in NaZSM-5.

6. Because we see no splitting or shift in the frequency of both the in-plane and the out-of-plane vibrations, it is evident that the occluded benzene molecules are not bonded directly to the framework sites or the extraframework cations of MCM-41. It is therefore likely that in analogy with the mode of packing in microporous materials, the benzene rings may align themselves in a direction parallel to the walls of MCM-41. The intermolecular spacing may, however, differ because of the difference in pore size and that in turn may decide the density of the encapsulated benzene.

The QENS results reveal that the benzene molecules confined in the MCM-41 possess mainly the translational motion in the energy domain of the present study. This observation is in contrast to the molecular motions of benzene in HZSM-5, where rotional motions were dominant under the identical experimental conditions, as is described in our earlier publication.[19] This corroborates our IR results that the dimensions of the confining medium control the motions of the occluded guest molecules. Thus, because the channel size in the case of ZSM-5 zeolite is comparable to the size of the benzene molecule, the translational motion gets restricted, giving rise to a highly compressed phase of occluded benzene. The restricted translational motion of benzene in the pores of ZSM5 zeolite has been reported by other workers also.[28] In the case of MCM-41, the large pore size of ∼35 Å facilitates the translational motion and therefore gives rise to a less compressed state of occluded benzene, as discussed later in detail.

A further comparison of IR data obtained for NaMCM-41 and NaZSM-5, both consisting of almost similar Si/Al ratios and also considering the results of all-silica and cation-exchanged MCM samples, rules out any specific interaction and coordination of occluded benzene molecules with zeolitic

framework sites. However, as discussed in refs 18 and 19 in detail, it is likely that the charges associated with the framework sites may assist in the formation of the initial layer and the adsorbate−adsorbate interaction may take over subsequently, leading thereby to stabilization of a clustered state of benzene within the channel system of a porous medium. The two-stage pore filling process, as seen in plots of Figure 4, tends to support this viewpoint. The results of the hydroxy region bands (Figure 7) reveal that the trapped benzene leads to a progressive decrease in the intensity of the 3740 cm^{-1} band due to isolated silanols. From the absorbance values given in this figure, the growth of a 3623 cm^{-1} band seems to have a bearance on the decrease in the intensity of 3740 cm^{-1} band. The appearance of a similar band at 3627 cm^{-1} and also a band at 3585 cm^{-1} have been reported by Jentys et al.[21] for the adsorption of benzene over MCM-41 at partial pressures between 10^{-2} and 1 mbar. These bands are assigned to the stretching vibrations of perturbed hydroxy groups formed by hydrogen bonding to benzene.[21] As has been discussed in our earlier publication in detail,[19] such a hydrogen bonding between OH groups and benzene molecules is expected to result in significant changes in the frequencies of in-plane C−H stretching vibrations of adsorbed benzene, which is contrary to the observations of this study. It is thus argued that the perturbation in ν(OH) groups may also occur due to the physical effect of the occluded compressed benzene, as discussed above. Due to large pore size of MCM-41, this perturbation is likely to be small and accordingly no bands are observed in the lower frequency region (i.e., 3500−3200 cm^{-1}), a feature commonly observed in the case of microporous zeolite such as ZSM-5.[22] This is in agreement with our contention that in their occluded state, the hexagonal plane of benzene molecules is parallel to the walls of MCM pores, causing no direct binding to the internal hydroxy groups.[18]

The results of our QENS and IR studies are in line with the process of capillary condensation of fluids in narrow pores. It is well reported that the average density of the capillary gas is usually larger than that of the bulk gas.[5] Discrepant opinions have, however, been reported in the case of capillary liquids. In some cases the density of the capillary liquids in pores is reported to be comparable with that of the bulk liquid.[29] On the other hand, recent studies reveal that when a liquid is placed in small pores, such as a porous vicor glass, the freezing point shifts to a lower value. This depression of freezing temperature is found to be inversely proportional to the pore radius.[6,7] Thus, using a picosecond time-resolved optical technique, Ritter et al.[6] demonstrated that this supercooled state is remarkably different from that of a free liquid and its temperature-independent collective response mimics that of a metastable solid state. Other researchers have similarly reported the pore size dependence of the relaxation time of the molecules placed in small cavities.[30]

Conclusions

The FTIR results of the present study reveal that the benzene occluded at room temperature in MCM-41 exists in an intermediate state that is denser than its liquid phase. The density and the dynamics of this state of benzene depend on the loading and the pore characteristics. The QENS study shows that whereas the benzene molecules possess only the rotational motion and negligible translational motion in the micropores of the ZSM-5 zeolite, in the case of MCM-41 the translational motion is dominant within the energy domain of the present study. The value of the diffusion constant arrived at from these data confirmed the condensation of benzene in the pores of MCM-41. Compared to ZSM5, a smaller fraction of dosed benzene gets trapped inside MCM-41 and this can be attributed to the greater translational mobility of the molecules in the two-dimensional array of nonconnecting cylindrical mesopores of the later sample. Further, the framework sites of MCM-41, such as Si or Al sites, OH groups, or the extraframework charge balancing cations, may play no significant role in the binding together and the dynamics of the above-mentioned transition state of benzene in the molecular sieve pores.

Acknowledgment. The encouragement and the support of Dr. J. P. Mittal, Director Chemistry and Isotope Group, to this study are gratefully acknowledged. Our thanks are due to Mr. K. T. Pillai of the Fuel Chemistry Division, BARC, for the measurements of surface area and pore size of molecular sieve samples. A.S. thanks the Department of Atomic Energy for a research fellowship.

References and Notes

(1) Corma, A. *Chem. Rev.* **1995**, *95*, 559.
(2) Zecchina, A.; Otero Arean, C. *Chem. Soc. Rev.* **1996**, 187.
(3) Knözinger, H.; Huber, S. *J. Chem. Soc., Faraday Trans.* **1998**, *94*, 2047.
(4) Ball, P. C.; Evans, R. *Langmuir* **1989**, *5*, 714.
(5) Evans, R.; Marconi, U. M. B.; Tarazona, P. *J. Chem. Soc., Faraday Trans.* **1986**, *82*, 1763, *J. Chem. Phys.* **1986**, *84*, 2376.
(6) Warnock, J.; Awschalom, D. D.; Shafer, M. W. *Phys. Rev. Lett.* **1986**, *57*, 1753. Ritter, M. B.; Awschalom, D. D.; Shafer, M. W. *Phys. Rev. Lett.* **1988**, *61*, 966.
(7) Mu, R.; Malhotra, V. M. *Phys. Rev. B* **1991**, *44*, 4296.
(8) Choudhary, V. R.; Nayak, V. S.; Choudhary, T. V. *Ind. Eng. Chem. Res.* **1997**, *36*, 1812.
(9) Wu, P.; Debebe, A.; Ma, Y. H. *Zeolites* **1983**, *3*, 118.
(10) Trombetta, M.; Armaroli, T.; Alejandre, A. G.; Solis, J. R.; Busca, G. *Appl. Catal. A: General* **2000**, *192*, 125.
(11) Primet, M.; Garbowski, E.; Mathieu, M. V.; Imelik, B. *J. Chem. Soc., Faraday I* **1980**, *76*, 1942.
(12) Su, B. L.; Manoli, J. M.; Potvin, C.; Barthomeuf, D. *J. Chem. Soc., Faraday Tans.* **1993**, *89*, 857.
(13) Kamble, V. S.; Gupta, N. M.; Kartha, V. B.; Iyer, R. M. *J. Chem. Soc., Faraday Trans. 1* **1993**, *89*, 1143.
(14) Shete, B. S.; Kamble, V. S.; Gupta, N. M.; Kartha, V. B. *J. Phys. Chem. B* **1998**, *102*, 5581.
(15) Shete, B. S.; Kamble, V. S.; Gupta, N. M.; Kartha, V. B. *Phys. Chem. Chem. Phys.* **1999**, *1*, 191.
(16) Kamble, V. S.; Gupta, N. M. *J. Phys. Chem. B* **2000**, *104*, 4588.
(17) Kamble, V. S.; Gupta, N. M. *Phys. Chem. Chem. Phys.* **2000**, *2*, 2661.
(18) Sahasrabudhe, A.; Kamble, V. S.; Tripathi, A. K.; Gupta, N. M. *J. Phys Chem. B* **2001**, *105*, 4374.
(19) Tripathi, A. K.; Sahasrabudhe, A.; Mitra, S.; Mukhopadhyay, R.; Gupta, N. M.; Kartha, V. B. *Phys. Chem. Chem. Phys.* **2001**, *3*, 4449.
(20) Mukhopadhyay, R.; Mitra, S.; Paranjpe, S.; Dasannacharya, B. A. *Nucl. Instrum. Methods A* **2001**, *474*, 45.
(21) Jentys, A.; Pham, N. H.; Vinek, H. *J. Chem. Soc., Faraday Trans.* **1996**, *92*, 3287.
(22) Armaroli, T.; Trombetta, M.; Alejandre, A. G.; Solis, J. R.; Busca, G. *Phys. Chem. Chem. Phys.* **2000**, *2*, 3341.
(23) Bée, M. *Quasielastic Neutron Scattering*; Adam-Hilger: Bristol, 1988.
(24) Press, W. *Single Particle Rotations in Molecular Crystals*; Springer: Berlin, 1981.
(25) Chudley, C. T.; Elliott, R. J. *Proc. Phys. Soc.* **1961**, *77*, 353.
(26) Rathbun, R. E.; Babb, A. L. *J. Phys. Chem.* **1961**, *65*, 1072.
(27) Winfield, D. J.; Ross, D. K. *Mol. Phys.* **1972**, *24*, 753.
(28) Zikanova, A.; Buelow, M.; Schlodder, H. *Zeolites* **1987**, *7*, 115.
(29) Machin, W. D. *Langmuir* **1994**, *10*, 1235.
(30) Brodka, A.; Zerda, T. W. *J. Chem. Phys.* **1992**, *97*, 5676. Zerda, T. W.; Shao, Y. *Chem Phys. Lett.* **1993**, *209*, 247.